Coherent Cherenkov-Cyclotron Radiation Excited by an Electron Beam in a Metamaterial Waveguide

J. S. Hummelt,* X. Lu, H. Xu, I. Mastovsky, M. A. Shapiro, and R. J. Temkin
Massachusetts Institute of Technology, 77 Massachusetts Avenue, Cambridge, Massachusetts 02139, USA
(Received 7 April 2016; published 2 December 2016)

An electron beam passing through a metamaterial structure is predicted to generate reversed Cherenkov radiation, an unusual and potentially very useful property. We present an experimental test of this phenomenon using an intense electron beam passing through a metamaterial loaded waveguide. Power levels of up to 5 MW are observed in backward wave modes at a frequency of 2.40 GHz using a one microsecond pulsed electron beam of 490 keV, 84 A in a 400 G magnetic field. Contrary to expectations, the output power is not generated in the Cherenkov mode. Instead, the presence of the magnetic field, which is required to transport the electron beam, induces a Cherenkov-cyclotron (or anomalous Doppler) instability at a frequency equal to the Cherenkov frequency minus the cyclotron frequency. Nonlinear simulations indicate that the Cherenkov-cyclotron mode should dominate over the Cherenkov instability at a lower magnetic field where the highest output power is obtained.

DOI: 10.1103/PhysRevLett.117.237701

An electron beam interacting with a metamaterial (MTM) structure generates Cherenkov radiation in the backward direction, which is the reverse of the forward traveling Cherenkov radiation generated in conventional media [1–4]. This property is of great fundamental interest, but it may also prove to be of value in applications such as detectors in particle physics [5] or in microwave generation [6–13]. There have been very few experiments on the generation of reversed Cherenkov radiation. One experimental observation was carried out using electron bunches from an accelerator passing through a metamaterial waveguide, producing emission in the left-handed frequency band of the MTM at 10 GHz [14]. A second experiment used a phased electromagnetic dipole array to simulate a moving charged particle beam, producing reversed Cherenkov radiation in the 8.1 to 9.5 GHz range [15]. These previous experiments, however, have not investigated the interaction of a continuous electron beam with a metamaterial structure, which is of great interest for sources of microwave generation. Our experiments show that when a magnetic field is used to transport the electron beam, the reverse Cherenkov instability is not the dominant effect observed. Instead, the Cherenkov-cyclotron instability dominates over the Cherenkov instability. This result has significant implications for any practical application of metamaterials in microwave generation.

High power microwave (HPM) sources are widely used in radar, defense, accelerator, and industrial applications; many examples are given in Refs. [16–18]. Modern particle in cell (PIC) codes have been developed that allow the design of HPM devices with full 3D treatment of both the electron beam and the electromagnetic wave [19,20]. Another important development are the advances in electromagnetics, including extensive research on novel photonic and metamaterial structures. These structures open up new possibilities for the design of HPM devices.

Metamaterials are artificial materials with carefully engineered dispersion displaying novel properties [21–24]. The most common manifestation of a MTM structure uses split-ring resonators (SRRs) formed on a dielectric substrate such as a printed circuit board. This approach, which was used in the previous reverse Cherenkov experiments [14,15], is not acceptable for high power microwave generation since the substrate will outgas and the SRRs will overheat. We have circumvented this limitation by using complementary-split-ring resonators (CSRRs) [25]. Figure 1 shows the design of the metamaterial structure investigated in our experiments. It is constructed by inserting two copper metamaterial plates machined with periodic single CSRRs in a waveguide. An electron beam propagates along the waveguide between the plates, centered on the axis.

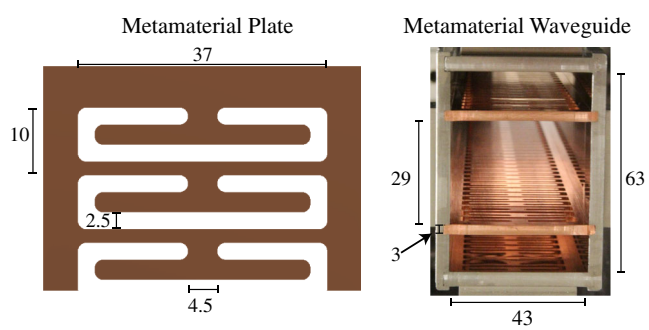

FIG. 1. A CAD rendering of one of the metamaterial plates (left) and a photograph of the fully assembled structure (right). Dimensions are in mm.

 © 2016 American Physical Society

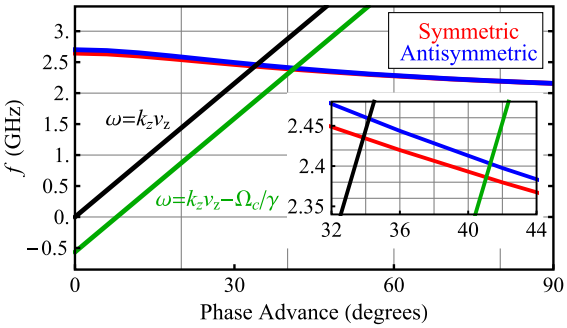

FIG. 2. Dispersion relation for the symmetric (red) and antisymmetric (blue) modes of the metamaterial structure with the Cherenkov (black) and anomalous Doppler (green) beam lines. The phase advance is $k_z p$ and $p = 10$ mm. The beam energy is 490 keV and the magnetic field 400 G.

The dispersion of the modes of the MTM loaded waveguide was calculated numerically using the eigenmode solver of CST Microwave Studio. The dispersion curves of the two lowest order modes are shown in Fig. 2. Two distinct modes are excited in the waveguide, a symmetric mode and an antisymmetric mode. The names symmetric ($E_{\text{transverse}} = 0$ on axis) and antisymmetric ($E_{\text{axial}} = 0$ on axis) are used because they describe the symmetry of the electric field components across a plane lying in the center of the waveguide and parallel to both metamaterial plates. They can also be understood as the superposition of two surface modes that exist on each of the metamaterial plates shown in Fig. 1. The symmetric mode occurs when two surface waves are in phase, and the antisymmetric mode occurs when they are 180 degrees out of phase. An important property of these modes is that they are below cutoff for TM modes in the 43-by-63-mm waveguide shown in Fig. 1, so the modes can only propagate in the guide due to the presence of the MTM plates.

Although our analysis uses numerical methods, we have shown that these MTM modes can be represented by an effective medium theory with the values of permeability and permittivity given by

$$\mu_{\text{eff}} = 1 - \frac{\omega_{\text{co}}^2}{\omega^2}, \qquad \epsilon_{\text{eff}} = 1 - \frac{\omega_p^2}{\omega^2 - \omega_0^2}, \tag{1}$$

where ω is the frequency, ω_{co} is the waveguide cutoff frequency for TM modes ($\omega_{co}/2\pi \sim 4.2$ GHz), ω_p is the effective plasma frequency of the medium ($\omega_p/2\pi \sim 1.7$ GHz), and ω_0 is the resonant frequency of the medium ($\omega_0/2\pi \sim 2.1$ GHz). The properties of the effective medium model are described in Refs. [8,25]. Although Eq. (1) is not used to analyze our data, it is helpful since it shows that both ϵ and μ are negative at the frequencies of interest, an important property for wave propagation in a metamaterial structure.

Figure 3 shows the experimental arrangement. The electron beam was generated by an electrostatically focused, 1-μs pulsed electron gun. Power generated by backward waves in the metamaterial structure is reflected at the gun end and is coupled out at the collector end in the two WR284 (rectangular waveguide 72.14 by 34.04 mm) output waveguides to high power loads (not shown in Fig. 3).

Previous theoretical analysis of the interaction of an electron beam with a metamaterial structure has only considered the possibility of backward (or reverse) Cherenkov radiation [6–13], which would lead to a backward wave oscillator (BWO) interaction [26]. However, we have found that it is also necessary to consider Cherenkov-cyclotron instabilities [27]. The general expression that describes both Cherenkov and Cherenkov-cyclotron instabilities is given by

$$\omega = k_z v_z + n\Omega_c/\gamma. \tag{2}$$

In Eq. (2) the frequency is ω, the axial wave number is k_z, v_z is the axial electron velocity, n is an integer, Ω_c is the

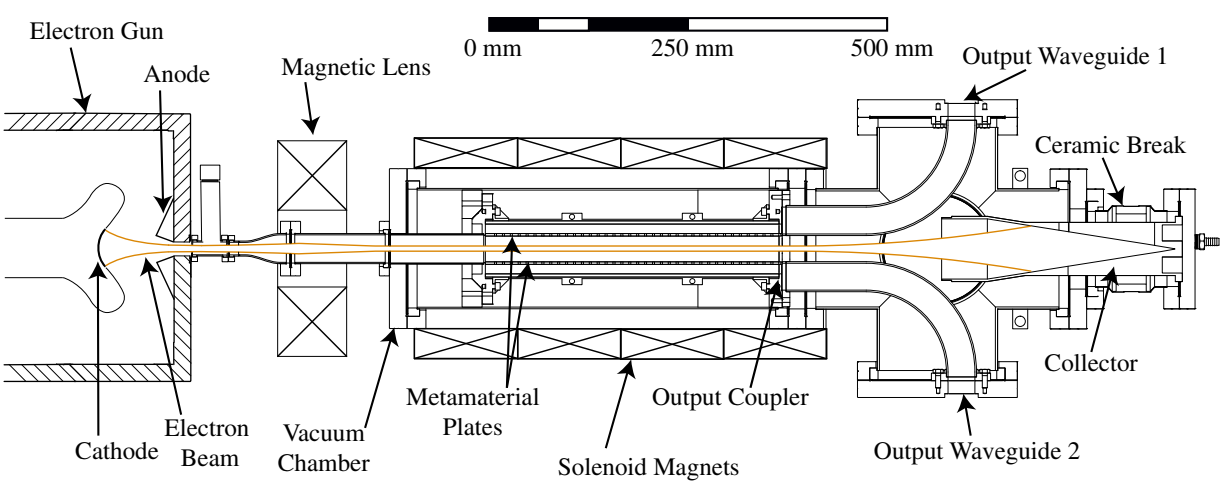

FIG. 3. Simplified schematic of the high power metamaterial experiment.

electron cyclotron frequency eB/m_e (with e, m_e the electron charge and rest mass), B is the magnetic field, and γ is the Lorentz factor equal to $(1 - v_z^2/c^2)^{-1/2}$, where c is the speed of light. In Eq. (2) the relation with $n = 0$ is the ordinary Cherenkov instability, and the relation with $n \neq 0$ is a Cherenkov-cyclotron instability, where the special case $n = -1$ is the anomalous Doppler instability.

A recent review and discussion of the Cherenkov-cyclotron instabilities in conventional BWOs for a range of values of the parameter n in Eq. (2) has been published by Nusinovich and Zhao [28]. In studies of such BWOs, the anomalous Doppler resonance can lead to enhanced efficiency and output power. Competition can also occur between resonances of different values of n when the resultant frequencies (ω) are nearly identical [28].

An instability, leading to microwave generation, may occur when both the line expressed by Eq. (2) and the dispersion curve intersect, as illustrated near 2.4 GHz in Fig. 2. At all of the intersections in Fig. 2, the group velocity, given by the derivative of the frequency with respect to the wave vector (or phase), is negative, indicating a backward (or reverse) wave. Instability leading to coherent microwave generation can occur at any of the four intersections shown in Fig. 2. In a Cherenkov instability, the wave grows due to the synchronism between the wave phase velocity and the electron beam velocity, $\omega/k_z = v_z$. In a Cherenkov-cyclotron instability, the phase synchronism is between the Doppler shifted phase of the wave and the cyclotron motion of the electron beam: $\omega - k_z v_z = -\Omega_c/\gamma$. In the MTM structure, the fields of the electromagnetic wave are not easily described by analytic theory, so we must rely on numerical codes for linear and nonlinear estimates of the strengths of these interactions.

The interaction of the electron beam with the modes of the metamaterial structure was studied using the PIC solver of CST Particle Studio for electron beam energies from 400 to 500 keV and magnetic fields of 350 to 5000 G. Sample simulation results are shown in Fig. 4. Figure 4(a) shows the electric field components and particle trajectories for $B_z = 1500$ G and for a 490 keV, 84 A electron beam. For these conditions, the symmetric mode is excited. The particle trajectories are close to the axis of the structure. The microwave output power, coupled into the two output waveguides, saturated at a total of 6.2 MW at 2.40 GHz. In the simulation, the symmetric mode was identified by the fact that the phase of the output microwaves was the same in the two output waveguides. The instability was identified as the Cherenkov instability because the frequency did not change as the magnetic field was varied.

Figure 4(b) shows the electric field components and particle trajectories for the case $B_z = 450$ G. In this case, the antisymmetric mode was excited. In the simulation, the beam is deflected off axis and spirals even though it has no initial transverse velocity. The beam spirals with an angular

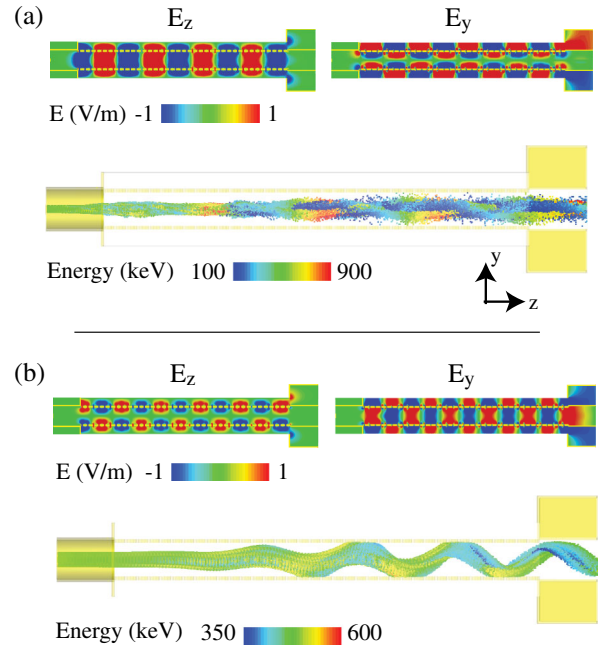

FIG. 4. PIC simulation of the metamaterial structure with a 490 keV 84 A electron beam showing the E_z and E_y field components and the particle orbits when the (a) symmetric mode is excited at 1500 G and the (b) antisymmetric mode is excited at 700 G.

frequency equal to the microwave output frequency (2.4 GHz). The predicted microwave power was 5.4 MW at 2.36 GHz. The instability was identified as the anomalous Doppler instability because the frequency changed as the magnetic field was varied in agreement with Eq. (2) for $n = -1$.

Figures 4(a) and 4(b) indicate that the bunching and energy extraction are significantly different for low vs high magnetic field. At high magnetic field, operating in the symmetric mode with a Cherenkov instability, the particles have a large energy dispersion during the bunching and energy extraction process. This is evident in Fig. 4(a) by the large energy spread of the particles in the simulation of the electron beam. At low magnetic field, in the antisymmetric mode with an anomalous Doppler instability, the particles gradually lose energy while maintaining a modest energy spread. This latter mechanism may be very promising in achieving very high efficiency if the structure is suitably tapered along the axis.

Experimental data were collected over a wide range of operating parameters, from 400 to 490 kV and 350 to 1600 G. An example of a high output power shot is shown in Fig. 5(b). For this shot, the magnetic field was 375 G, the voltage was near 400 kV and the current was 62 A. The output power averaged over the central portion of the pulse was 2.4 MW. The measured frequency was 2.38 GHz. The measured phase in the two output arms showed that the antisymmetric mode was excited. Tuning of the frequency with magnetic field, as explained in more detail below,

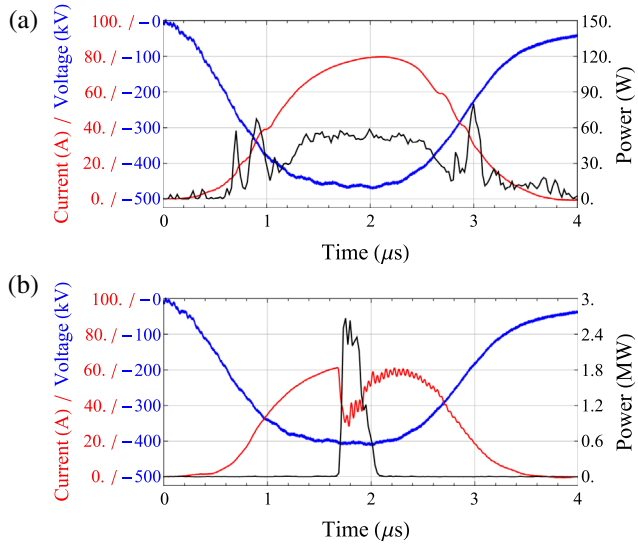

FIG. 5. Microwave power (black), electron gun voltage (blue), and measured collector current (red) for an applied magnetic field of (a) 1500 G and (b) 375 G.

indicated that the anomalous Doppler instability was excited.

Figure 5(b) shows that the excitation of the high power microwave output was coincident with interception of the electron beam on the metamaterial circuit. In Fig. 5(b), the collector current, which rises with voltage, reaches 60 A at a voltage of 400 kV at about 1.6 μs. The microwave power then increases to about 2.7 MW. The collector current simultaneously drops since part of the beam, about 50%, is intercepted on the metamaterial plates. The beam interception is caused by the excitation of the antisymmetric mode at high power, which results in the electron beam striking the metamaterial plates, as seen in Fig. 4(b). As the voltage decreases, the mode goes out of resonance and the electron beam is again transmitted to the collector. High output power, at the megawatt level, was only achieved in the experiments when the device was operated at low magnetic field values, below 450 G. The antisymmetric mode was always excited at those magnetic field values, with significant electron beam interception in all cases, in agreement with the PIC code simulations. Although the beam was intercepted on the metamaterial plates, inspection of the plates after operation showed no visible damage. There was also no evidence of breakdown during these high power shots. It is possible that tapering the spacing of the metamaterial plates could reduce this interception in future experiments. The highest output power levels, up to 5 MW, were observed at low magnetic field values with pulse widths of 100 to 400 ns.

In contrast, Fig. 5(a) shows a shot at a high magnetic field, with wide pulses of microwave emission in the symmetric mode with no electron beam interception. The output power is approximately 50 W, which is 5 orders of magnitude below the power level seen at lower magnetic field, which may be characteristic of a pre-oscillation condition. The low power level of the symmetric modes has no clear explanation at this time.

A summary of the experimental results as a function of the solenoidal magnetic field is shown in Fig. 6. For these results, the voltage was 490 kV and the current 84 A. Figure 6(a) shows the relative phase $\Delta\phi$ in the two output waveguides vs magnetic field. It demonstrates that as the magnetic field increases, the output mode switches from the antisymmetric mode ($\Delta\phi = 180$ degrees) to the symmetric mode ($\Delta\phi = 0$) at about 750 G. This result is in very good agreement with CST PIC code simulations. Figure 6(b) shows the output power vs magnetic field. From 350 to 450 G, the output power levels are in the megawatt power range, in very good agreement with predictions from the CST PIC code. However, above 450 G, the output power drops by 4 orders of magnitude, consistent with emission of incoherent radiation. As shown in Fig. 6(a), the antisymmetric mode was excited from 350 to 750 G and the symmetric mode from 750 to 1500 G. Therefore, the low output power was in the antisymmetric mode from 450 to 750 G and the symmetric mode from 750 G to 1500 G. Some of the CST PIC simulations showed that the

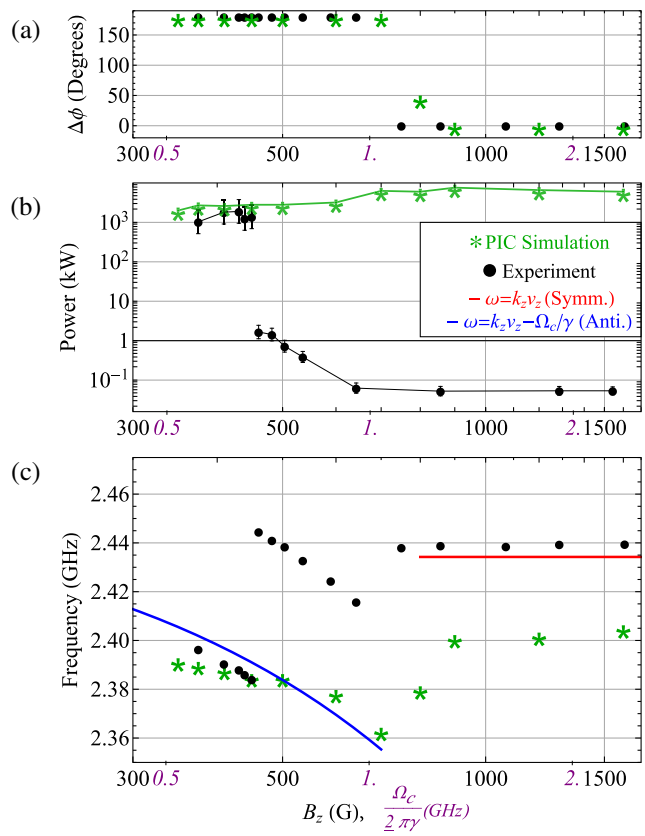

FIG. 6. Measured (black) and simulated (green) (a) $\Delta\phi$, (b) microwave power, and (c) frequency. In addition, the red line is the symmetric mode Cherenkov instability ($\omega = k_z v_z$), and the blue line is the antisymmetric mode Cherenkov-cyclotron instability ($\omega - k_z v_z = -\Omega_c/\gamma$).

microwave output power could remain in a pre-oscillation state for a long time prior to the onset of coherent radiation and transition to a high output power level after several hundred nanoseconds. It is possible that operation with a longer pulse length could excite the modes. There is some evidence for this in the decreasing power with magnetic field seen in the low power results in Fig. 6(b). Alternatively, the codes may not be adequate in the regimes where low power was observed.

Figure 6(c) shows the frequency vs magnetic field. The output frequency was very narrow band, with a 3 dB bandwidth of a few MHz or less in all cases. As shown in Fig. 6(c), at lower magnetic field values between 350 and 475 G, where the power levels agree reasonably well with CST PIC code theory predictions, the frequencies are also in good agreement with theory. From about 475 to 750 G, the observed frequency tunes with magnetic field, as expected for the Cherenkov-cyclotron instability, but the observed frequencies are about 60 MHz higher than CST predictions. This discrepancy can be explained by the fact that the CST code also predicts high output power in this frequency range, while only low power was observed. High power operation causes a large shift in the operating frequency due to dispersion of the wave by the electron beam when operating in the nonlinear regime. Since the device did not reach high output power, the dispersive effects were reduced, which could account for the 60 MHz offset. Above 750 G, the frequency is constant, with no observation of frequency tuning with magnetic field, consistent with the Cherenkov instability.

In summary, this paper reports the first experimental demonstration of coherent microwave generation from a continuous electron beam interacting with a metamaterial structure. The metamaterial loaded structure may prove promising for high power microwave generation. It has the attractive feature of being very compact since the MTM loaded waveguide is below cutoff. This may prove useful in high power microwave generation at lower frequencies, where many accelerators and transmitters operate. In the planar form demonstrated in these experiments, the metamaterial can be easily machined from a solid plate. Operation in the anomalous Doppler regime with a tapered structure could lead to a simple, high efficiency radiator.

The authors gratefully acknowledge Dr. Jake Haimson for helpful discussions. This research was supported by the Air Force Office of Scientific Research within the Multidisciplinary University Research Initiative under Grant No. FA9550-12-1-0489 through the University of New Mexico.

*jshummelt@gmail.com

[1] V. G. Veselago, Sov. Phys. Usp. **10**, 509 (1968).
[2] N. Seddon and T. Bearpark, Science **302**, 1537 (2003).
[3] J. Chen, Y. Wang, B. Jia, T. Geng, X. Li, L. Feng, W. Qian, B. Liang, X. Zhang, M. Gu, and S. Zhuang, Nat. Photonics **5**, 239 (2011).
[4] A. Grbic and G. V. Eleftheriades, J. Appl. Phys. **92**, 5930 (2002).
[5] V. Ginis, J. Danckaert, I. Veretennicoff, and P. Tassin, Phys. Rev. Lett. **113**, 167402 (2014).
[6] Y. P. Bliokh, S. Savel'ev, and F. Nori, Phys. Rev. Lett. **100**, 244803 (2008).
[7] M. A. Shapiro, S. Trendafilov, Y. Urzhumov, A. Alu, R. J. Temkin, and G. Shvets, Phys. Rev. B **86**, 085132 (2012).
[8] J. S. Hummelt, S. M. Lewis, M. A. Shapiro, and R. J. Temkin, IEEE Trans. Plasma Sci. **42**, 930 (2014).
[9] D. M. French, D. Shiffler, and K. Cartwright, Phys. Plasmas **20**, 083116 (2013).
[10] D. Shiffler, J. Luginsland, D. M. French, and J. Watrous, IEEE Trans. Plasma Sci. **38**, 1462 (2010).
[11] Z. Duan, J. S. Hummelt, M. A. Shapiro, and R. J. Temkin, Phys. Plasmas **21**, 103301 (2014).
[12] N. A. Estep, A. N. Askarpour, S. Trendafilov, G. Shvets, and A. Alu, IEEE Trans. Antennas Propag. **62**, 3212 (2014).
[13] S. Galyamin, A. Tyukhtin, A. Kanareykin, and P. Schoessow, Phys. Rev. Lett. **103**, 194802 (2009).
[14] S. Antipov, L. Spentzouris, W. Gai, M. Conde, F. Franchini, R. Konecny, W. Liu, J. G. Power, Z. Usof, and C. Jing, J. Appl. Phys. **104**, 014901 (2008).
[15] S. Xi, H. Chen, T. Jiang, L. Ran, J. Huangfu, B. Wu, J. Kong, and M. Chen, Phys. Rev. Lett. **103**, 194801 (2009).
[16] J. Benford, J. A. Swegle, and E. Schamiloglu, *High Power Microwaves*, 2nd ed. (Taylor and Francis Group, LLC, Baltimore, MD, 2007).
[17] R. J. Barker and E. Schamiloglu, *High-Power Microwave Sources and Technologies*, 2nd ed. (IEEE Press, Piscataway, NJ, 2001).
[18] S. H. Gold and G. S. Nusinovich, Rev. Sci. Instrum. **68**, 3945 (1997).
[19] C. K. Birdsall and A. B. Langdon, *Plasma Physics via Computer Simulation* (Taylor & Francis, New York, 2004).
[20] R. W. Hockney and J. W. Eastwood, *Computer Simulation Using Particles* (Taylor & Francis, New York, 1988).
[21] J. B. Pendry, A. J. Holden, W. J. Stewart, and I. Youngs, Phys. Rev. Lett. **76**, 4773 (1996).
[22] J. B. Pendry, A. J. Holden, D. J. Robbins, and W. J. Stewart, IEEE Trans. Microwave Theory Tech. **47**, 2075 (1999).
[23] D. R. Smith, W. J. Padilla, D. C. Vier, S. C. Nemat-Nasser, and S. Schultz, Phys. Rev. Lett. **84**, 4184 (2000).
[24] D. R. Smith and N. Kroll, Phys. Rev. Lett. **85**, 2933 (2000).
[25] F. Falcone, T. Lopetegi, M. A. G. Laso, J. D. Baena, J. Bonache, M. Beruete, R. Marques, F. Martin, and M. Sorolla, Phys. Rev. Lett. **93**, 197401 (2004).
[26] S. E. Tsimring, *Electron Beams and Microwave Vacuum Electronics* (John Wiley and Sons, Hoboken, New Jersey, 2007).
[27] G. S. Nusinovich, *Introduction to the Physics of Gyrotrons*, 1st ed. (John Hopkins University Press, Baltimore, MD, 2004).
[28] G. S. Nusinovich and D. Zhao, IEEE Trans. Plasma Sci. **43**, 804 (2015).